CHEMISTRY
A EUROPEAN JOURNAL

DOI: 10.1002/chem.200700236

Investigation of an Acid–Base and Redox Molecular Switch: From Bulk to the Single-Molecule Level

Rabih O. Al-Kaysi,[a] José Luis Bourdelande,[b] Iluminada Gallardo,[b] Gonzalo Guirado,*[b] and Jordi Hernando*[b]

Abstract: In this work we investigate a new fluorescent molecular switch based on the interconversion between the fluorescent zwitterionic form (ZW1) and the non-fluorescent anionic state (MC2) of a spirocyclic Meisenheimer complex of 1,3,5-trinitrobenzene. Density functional theory molecular orbital calculations reveal that photo-induced electron transfer from a guanidine group to the trinitrocyclohexadiene fluorophore of the complex quenches the emission from MC2. Protonation, as well as coordination of other Lewis acids to the guanidine group, suppress the quenching mechanism and allow the complex to fluoresce. In agreement with the calculations, reversible on–off fluorescence switching of the ZW1–MC2 bulk system occurs by protonation–deprotonation of the guanidine moiety upon acid–base addition. Interestingly, spectroelectrochemical ensemble measurements show that switching of the ZW1–MC2 pair can also be attained electrochemically, thus unraveling the versatile functioning of this system. The ultimate limit of monitoring the reversible on–off operation of individual switch molecules is reached by means of single-molecule fluorescence spectroscopy, which demonstrates the potential of the ZW1–MC2 system to be used as a true single-molecule switch on the nanometer scale.

Keywords: electron transfer · Meisenheimer complex · molecular switch · single-molecule studies · zwitterionic complex

Introduction

The design, synthesis, and characterization of molecular switches has become an active area of research in recent decades.[1] Molecular systems, the properties of which can be modulated between two different stable states in a controlled and reversible manner, have emerged as promising materials for the construction of chemical and biological sensors,[2] as well as of true molecular memories[3] and devices.[4] Ultimately, the development of molecular switches to be operated in such nanometer-sized constructs requires addressing and evaluating their performance down to the molecular level.[5] Due to its sensitivity and non-invasive character, fluorescence detection of molecular switches appears to be an ideal tool to reach this limit.[6]

Indeed, single-molecule fluorescence spectroscopy (SMS) has largely been proved to be capable of monitoring the optical behavior of individual molecular systems.[7] Hence, much effort has been devoted in recent times to developing and discovering fluorescent molecular switches that are addressable at the single-molecule level. However, the number of such molecular switches shown to work under ambient conditions is still limited. Reversible single-molecule fluorescence photoswitching of diarylethene derivatives,[8] commercial carbocyanine molecules[9,10] and GFP-like proteins[11,12] has been demonstrated only recently. At the same time, reversible switching of individual fluorescent molecules upon a chemical stimulus has also been reported,[13–16] opening the door to performing sensing at the nanometer scale. Thus, pH-induced modulation of the emission from single seminaphtorhodafluor chromophores has been described,[14] whereas switching of individual fluorescent perylenediimide molecules, containing free amines, has been attained by using protonation–deprotonation processes and Lewis acid coordination.[15] The development of such single-molecule probes must eventually allow monitoring of individual reactive events in relevant chemical and biological processes.[17]

[a] Dr. R. O. Al-Kaysi
Department of Chemistry, University of California
Riverside, CA 92521 (USA)

[b] Prof. J. L. Bourdelande, Prof. I. Gallardo, Dr. G. Guirado, Dr. J. Hernando
Departament de Química, Universitat Autònoma de Barcelona
08193 Cerdanyola del Vallès (Spain)
Fax: (+34) 93-581-1265
E-mail: gonzalo.guirado@uab.es
jordi.hernando@uab.es

Recently we reported the synthesis of a new fluorescent system: the zwitterionic spirocyclic Meisenheimer complex of 1,3,5-trinitrobenzene (ZW1, Scheme 1).[18] Although the

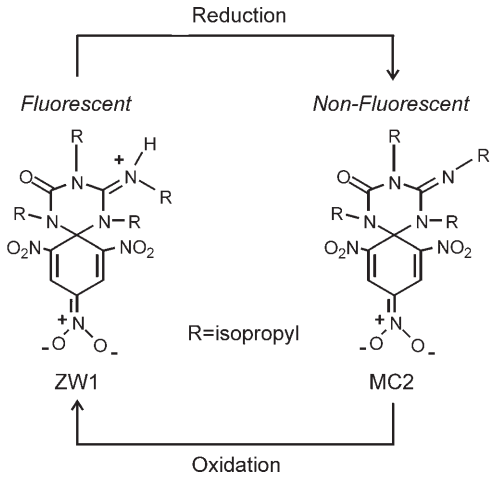

Scheme 1. Electrochemical redox interconversion between the zwitterionic (ZW1, fluorescent) and anionic (MC2, non-fluorescent) Meisenheimer complexes of 1,3,5-trinitrobenzene.

intermediates of nucleophilic aromatic substitutions in polynitroaromatic compounds, the so-called Meisenheimer complexes, are known to be unstable and poorly fluorescent,[19,20] ZW1 can be isolated as a stable red-orange solid whose fluorescence quantum yield in solution is significantly high ($\Phi_f = 0.5$).[18] More noticeably, ZW1 shows interesting electrochemical behavior, which is summarized in Scheme 1.[21] One-electron reduction of ZW1 yields a non-fluorescent, anionic Meisenheimer complex (MC2, Scheme 1), where the guanidine moiety of the triazine ring is deprotonated. Subsequent one-electron oxidation of MC2 allows recovery of the fluorescent ZW1 species.[21] Together with the large Φ_f value measured for the zwitterionic form of the Meisenheimer complex, the electrochemical interconversion cycle revealed allows the ZW1–MC2 system to be envisaged as a potential single-molecule fluorescent switch.

In this contribution we study both experimentally and theoretically the performance of the ZW1–MC2 system as a fluorescent molecular switch. First, theoretical calculations are performed to investigate the origin of the different optical properties of ZW1 and MC2, thus uncovering the underlying mechanism accounting for their switching behavior. Spectroscopic and spectroelectrochemical measurements in the bulk are then performed to address the switching response of the ZW1–MC2 pair upon two different stimuli: chemical protonation–deprotonation of the guanidine group, and electrochemical redox interconversion. To assess the potential of the ZW1–MC2 system to operate as a single-molecule fluorescent switch, we finally examine the controlled and reversible on-off switching of its luminescence at the single-molecule level by means of SMS.

Results and Discussion

Synthesis and optical properties: The synthesis of Meisenheimer complexes ZW1[18] and MC2[21] has already been reported. Both compounds are *spiro* adducts of a negatively-charged trinitrocyclohexadiene group and a triazene ring, which are therefore expected to be perpendicularly oriented in the ground electronic state of ZW1 and MC2. Protonation–deprotonation of the guanidine moiety in the traizene ring leads to formation of either ZW1 or MC2 (see Scheme 1).

Figure 1 depicts the absorption and fluorescence spectra of pure ZW1 and the potassium salt of MC2 in acetonitrile. Both ZW1 and MC2 solutions display similar absorption

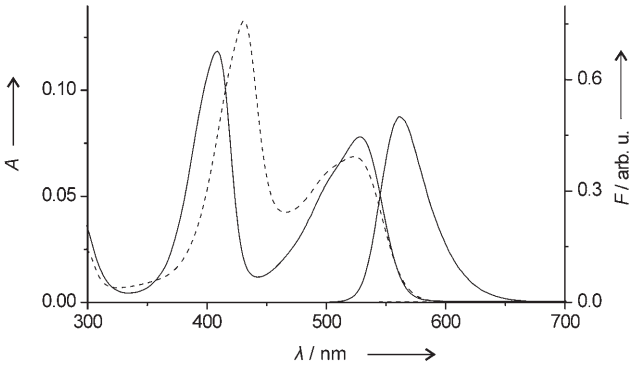

Figure 1. Absorption (A) and fluorescence (F) emission spectra of ZW1 (solid) and the potassium salt of MC2 (dashed) in acetonitrile ($c_{ZW1} = c_{MC2} = 5 \times 10^{-6}$ M, $\lambda_{exc} = 408$ nm). Due to its low Φ_f, the fluorescence spectrum of MC2 is not visible in the figure.

bands at about 410 nm and about 530 nm, the lower wavelength absorbance showing the higher intensity. Such spectral features are characteristic of trinitrocyclohexadiene moieties in anionic Meisenheimer complexes.[22] In agreement with the theoretical calculations discussed below, this suggests that the ground electronic state absorption of the trinitrocyclohexadiene group in ZW1 and MC2 is not significantly affected by the presence of a close orthogonally oriented triazene unit.

In spite of their similar absorption behavior, ZW1 and MC2 show opposite fluorescence properties (Figure 1). Although Meisenheimer complexes are, in general, expected to be poorly fluorescent due to the presence of the strong electron-withdrawing nitro groups,[20] strong fluorescence emission is detected upon excitation of ZW1 at either 406 or 526 nm ($\lambda_{max} = 563$ nm and $\Phi_f = 0.5$ in acetonitrile). Conversely, a very minor fluorescence signal is detected for MC2 under the same conditions ($\Phi_f < 0.01$), even though the optically excited trinitrocyclohexadiene groups of both ZW1 and MC2 do not show apparent structural differences.

Theoretical calculations: Quantum-chemical calculations were carried out to reveal the origin of the different fluorescent behavior of ZW1 and MC2. For this purpose we per-

formed density functional theory (DFT) and time-dependent density functional theory (TD-DFT) calculations, employing the B3LYP hybrid functional and the 6–31G(d,p) and 6–311+G(d,p) basis sets. In agreement with the X-ray diffraction structure resolved for ZW1,[23] B3LYP/6–31G-(d,p) geometry optimizations of the ZW1 and MC2 ground electronic states show a nearly perpendicular arrangement of their constituent trinitrocyclohexadiene and triazene units. Strong electronic coupling between these groups is therefore prevented in the ZW1 and MC2 ground states, in which the molecular orbitals must then be localized on either the trinitrocyclohexadiene moiety or the triazene ring. This situation is illustrated clearly by Figure 2, which displays the highest occupied molecular orbitals (HOMOs) of ZW1 and MC2, localized on each of their two constituent units.

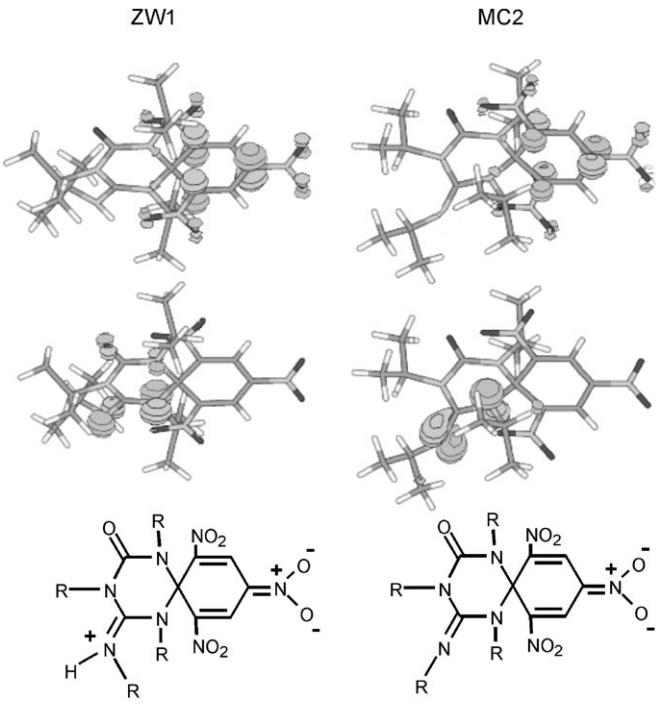

Figure 2. Highest occupied molecular orbitals of ZW1 and MC2 which are localized on each of the two constituent units of the complex: the trinitrocyclohexadiene ring (top) and the triazene moiety (bottom). Molecular orbital calculations have been performed at the B3LYP/6–311+G-(d,p) level on the B3LYP/6–31G(d,p) optimal geometry and accounting for the acetonitrile solvent.

Table 1 displays the energies and relative intensities of the UV/Vis absorption bands computed for ZW1 and MC2 by means of TD-DFT at the B3LYP/6–311+G(d,p) level on the B3LYP/6–31G(d,p) optimal geometries, and accounting for the acetonitrile solvent. A notably reasonable agreement with the experimental data is encountered. Thus, deviations lower than 15% in transition energy and 14% in relative intensity are found between the theoretical and experimental results. A detailed analysis of the optically active absorption transitions of ZW1 and MC2 calculated theoretically reveals

Table 1. Energies and relative intensities of the UV/Vis absorption bands of ZW1 and MC2.

		λ_1 [nm]	λ_2 [nm]	I_1/I_2[a]
ZW1	TD-DFT[b]	384	461	1.63[c]
	experimental	408	528	1.44
MC2	TD-DFT[b]	408	470	2.01[d]
	experimental	432	524	1.93

[a] Ratio of the computed oscillator strengths (f) for both absorption bands (TD-DFT) and ratio of the absorption extinction coefficients at the maxima of both bands (experimental). [b] B3LYP/6–311+G(d,p) level on the B3LYP/6–31G(d,p) ground electronic state optimal geometries and accounting for acetonitrile solvent. [c] $f_1=0.32$ and $f_2=0.19$. [d] $f_1=0.23$ and $f_2=0.11$.

that the molecular orbitals involved are localized mainly on the trinitrocyclohexadiene unit of these compounds. This explains why the ground electronic state absorptions of ZW1 and MC2 resemble those of isolated anionic trinitrocyclohexadiene complexes.

Further analysis of the molecular orbitals of ZW1 and MC2 was performed to investigate the different fluorescent properties of these compounds. Special attention was paid to the HOMOs and the corresponding lowest unoccupied molecular orbitals (LUMOs), localized on each of the constituent units of the complexes. The energies of these orbitals are plotted in Figure 3. For both ZW1 and MC2, the

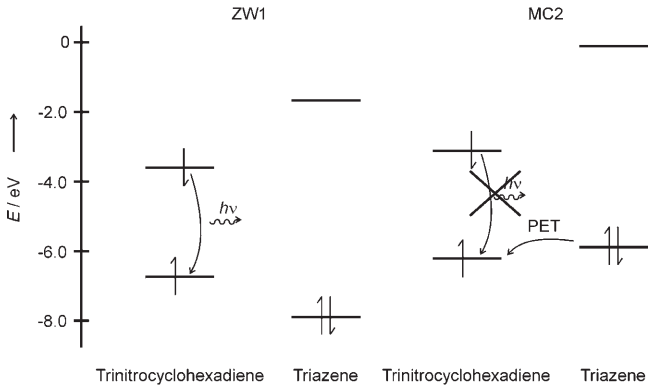

Figure 3. B3LYP/6–311+G(d,p) energies of the HOMOs and LUMOs of the trinitrociclohexadiene and triazene units of both ZW1 and MC2 in acetonitrile. The position of the valence electrons after light absorption is indicated, as well as the quenching mechanism accounting for the non-fluorescent behavior of MC2.

lowest energy LUMO is localized on the trinitrocyclohexadiene group, from which fluorescence emission should eventually arise. In contrast, the energy distribution of the HOMO orbitals dramatically changes from ZW1 to MC2 in acetonitrile. Whereas the highest energy HOMO in ZW1 is localized on the trinitrocyclohexadiene unit, the HOMO of the triazine ring in MC2 falls between the HOMO and LUMO of the trinitrocyclohexadiene moiety. In view of this fact, we conclude that the emissive behavior of ZW1 mainly depends on the intrinsic fluorescent properties of the trini-

trocyclohexadiene unit, a fluorophore group with $\Phi_f = 0.5$ in acetonitrile. Conversely, the molecular orbital diagram computed for MC2 suggests the occurrence of a competitive non-radiative pathway for excited state relaxation of the trinitrocyclohexadiene unit in this molecule: the photoinduced electron transfer (PET) from the HOMO of the triazene ring to the HOMO of the trinitrocyclohexadiene moiety (see Figure 3). If the rate of such intramolecular electron transfer becomes comparable or larger than the radiative decay rate of the excited state, deactivation of the fluorescence emission results.

PET is indeed a well-known fluorescence quenching mechanism, which has already been used in the design and synthesis of fluorescent probes and switches.[2,15,24–26] To be thermodynamically favorable, PET requires the energy of the HOMO of the electron donor group to fall above the energy of the HOMO of the nearby fluorophore unit that will eventually receive the transferred electron.[15,24–26] Therefore, MC2 in acetonitrile solution can display intramolecular photoinduced electron transfer from the triazene ring (electron donor) to the trinitrocyclohexadiene group (fluorophore), leading to a very efficient deactivation of the fluorescence emission of this species (see Figure 3). Lowering the energy of the HOMO of the electron donor by chemical modification of the triazene ring may prevent the PET process from occurring, thus recovering the fluorescent properties of the system. As already discussed, this is achieved in ZW1 upon protonation of the guanidine moiety in the triazene unit.

Acid–base fluorescence switching: Quantum-mechanical calculations indicate that the fluorescent behavior of the ZW1–MC2 pair can be modulated by protonation–deprotonation of the guanidine moiety in the complex. Herein we explored this switching mechanism by monitoring the absorption and emission spectra of the system upon addition of base (tetrabutylammonium hydroxide) and acid (perchloric acid). Measurements were performed in acetonitrile solution since this is a polar non-protic solvent in which both the ZW1–MC2 pair and the acid and base employed[27] are soluble and stable. Moreover, the use of deuterated acetonitrile also allowed us to follow the acid–base titration by NMR spectroscopy.

Figure 4 shows the variation of the absorption spectrum of ZW1 in acetonitrile upon addition of tetrabutylammonium hydroxide. Clearly, titration with a base results in the disappearance of ZW1 and the appearance of MC2 absorption bands. Eventually, quantitative deprotonation of ZW1 is achieved, thus recovering the absorption spectrum of pure MC2. The base-driven transformation of ZW1 into MC2 can also be revealed by fluorescence measurements, as illustrated in Figure 4. Titration of ZW1 in acetonitrile with tetrabutylammonium hydroxide gives rise to a decrease of the emission signal detected due to the non-fluorescent behavior of the resulting MC2 species. Thus, full conversion of ZW1 into MC2 finally leads to a nearly complete suppression of the emission arising from the sample.

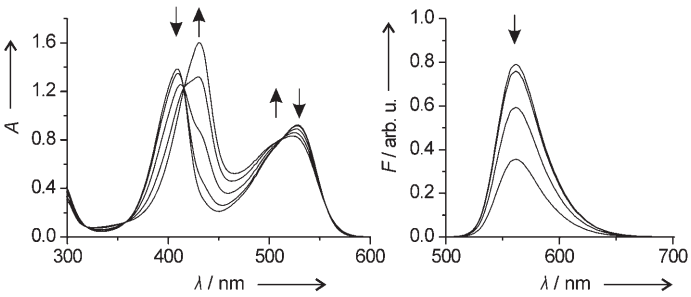

Figure 4. Absorption (*A*, left) and fluorescence (*F*, right) spectrophotometric titrations of ZW1 in acetonitrile with a solution of tetrabutylammonium hydroxide in isopropanol. The arrows indicate the evolution of the spectral bands for base/ZW1 molar ratios of 0, 0.25, 0.5, 0.75 and 1.0 (absorption, $c_{ZW1} = 4.2 \times 10^{-5}$ M) and 0, 0.1, 0.25, 0.5 and 1.0 (fluorescence, $c_{ZW1} = 2.8 \times 10^{-6}$ M). Note that equimolar addition of base results in the suppression of nearly all emission from the sample and, consequently, no fluorescence spectrum is visible in this case in the figure.

Operation of the ZW1–MC2 pair as a true molecular switch requires the base-driven transformation of ZW1 into MC2 to be reversible. Consequently, we monitored the changes in the absorption and fluorescence spectra of the previously base-titrated ZW1 solution upon $HClO_4$ addition. The results obtained are depicted in Figure 5, which clearly

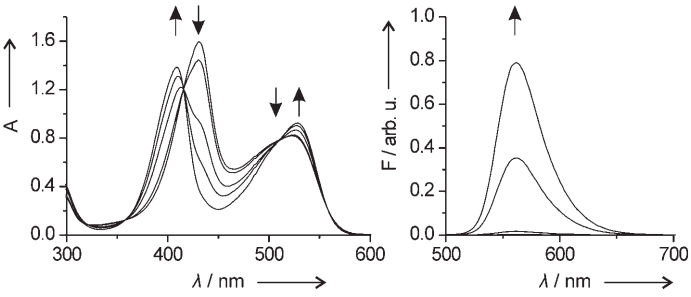

Figure 5. Absorption (*A*, left) and fluorescence (*F*, right) spectrophotometric titrations of the previously base-titrated solution of ZW1 in acetonitrile with perchloric acid in dioxane. The arrows indicate the evolution of the spectral bands for acid/MC2 ratios of 0, 0.2, 0.4, 0.8 and 1.0 (absorption, $c_{ZW1} = 4.2 \times 10^{-5}$ M) and 0, 0.1, 0.4 and 1.0 (fluorescence, $c_{ZW1} = 2.8 \times 10^{-6}$ M). After equimolar addition of acid, more than 99% of the fluorescence intensity of the original ZW1 sample is recovered.

show that titration with acid results in the protonation of MC2 to yield ZW1 again. Noticeably, both the absorption and fluorescence properties of the initial ZW1 sample are fully recovered after equimolar addition of acid. Therefore, the controlled and reversible acid–base fluorescent switching of the ZW1–MC2 system is demonstrated by our spectrophotometric measurements.

Up to five cycles of reversible on-off fluorescence switching of the same ZW1–MC2 solution have been successfully attempted without degradation of the sample. Nonetheless, careful control of the addition of acid and base to the system must be taken. Addition of an excess of tetrabutylammonium hydroxide leads to a new absorption band at

491 nm, which we ascribe to the irreversible product arising from the nucleophilic attack of the excess of base (i.e. OH^-) to the *spiro* position of the MC2 complex. This problem can be avoided if a non-nucleophilic base is employed, such as 1,4-diazabicyclo[2.2.2]octane (DABCO) or triethylamine. Due to the weaker basic character of these species, however, even the use of a large excess of base does not guarantee the full conversion of ZW1 into MC2. Analogously, an excess of perchloric acid in the sample leads to degradation of the Meisenheimer complexes, which may result from the protonation and subsequent descomposition of the nitro groups in the molecule.[28]

Fluorescence sensing of Lewis acids: In addition to protonation of the guanidine unit, the occurrence of PET and, therefore, fluorescence quenching in MC2, may also be prevented by coordination of other Lewis acids to the nitrogen atom of the imine group of the complex. Indeed, titration of a solution of MC2 in acetonitrile with triphenylborane, TiO_2, $FeCl_2$, or $Co(ClO_4)_2$ gives rise to the recovery of the fluorescence properties of the system, as illustrated in Figure 6.

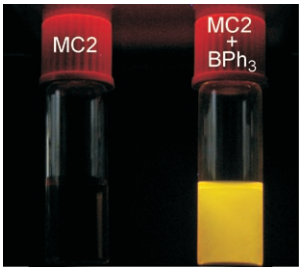

Figure 6. Fluorescence emission arising from a solution of MC2 in acetonitrile ($c = 1 \times 10^{-5}$ M) before (left) and after (right) addition of one equivalent of triphenylborane (irradiation with a UV lamp at 254 nm).

This indicates a decrease in the energy of the triazene ring HOMO upon MC2–Lewis acid adduct formation, which suppresses electron transfer to the excited trinitrocyclohexadiene unit, and thus allows the system to fluoresce. As previously observed for free-amine-containing perylenediimide molecules,[15,29] MC2 can therefore be employed not only as a proton fluorescent probe, but also as a chemical sensor for several other species.

Electrochemical redox fluorescence switching: Recently we investigated the redox properties of both ZW1 and MC2 by means of cyclic voltammetry and controlled potential electrolysis (see Scheme 1).[21] We observed that one-electron reduction of ZW1 in acetonitrile at $E° = -0.85$ V versus SCE produces the radical anion $ZW1^{-\bullet}$, which subsequently loses a hydrogen atom to yield MC2 with a rate constant of $78\ s^{-1}$.[21] Analogously, one-electron oxidation of MC2 in acetonitrile at $E° = 1.20$ V versus SCE gives rise to the formation of the radical cation $MC2^{+\bullet}$, which then abstracts an hydrogen atom from the solvent to yield ZW1, with a rate constant of $2 \times 10^6\ s^{-1}$.[21] Therefore, reversible protonation/deprotonation of the ZW1–MC2 system can be electrochemically induced even in a non-protic solvent such as acetonitrile. Since here we are concerned with the fluorescent switching behavior of the ZW1–MC2 pair, in this work the reversible electrochemical interconversion between ZW1 and MC2 is further analyzed by monitoring the changes in absorption and fluorescence spectra while applying controlled amounts of current at a given potential.

Figure 7 depicts the results obtained in our spectroelectrochemical measurements for a solution of ZW1 in acetonitrile. Clearly, application of a controlled reduction potential

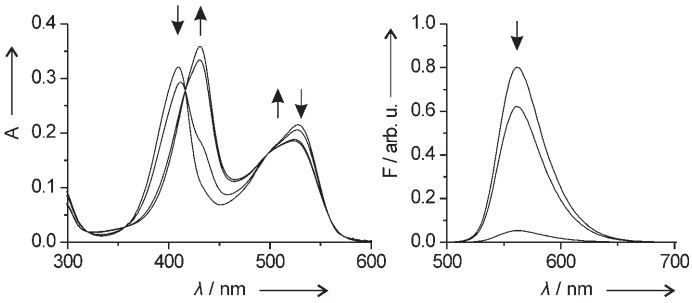

Figure 7. Absorption (A, left) and fluorescence (F, right) spectroelectrochemistry measurements of ZW1 in acetonitrile at a controlled reduction potential of −0.9 V versus SCE. The arrows indicate the evolution of the spectral bands upon application of 0, 0.4, and 0.9 (absorption) and 0, 0.45, 0.9, and 1 F (fluorescence) ($c_{ZW1} = 1.3 \times 10^{-5}$ M). Note that passage of 1 F results in the suppression of nearly all emission from the sample and, consequently, no fluorescence spectrum is visible in the figure in this case.

to the sample ($E = -0.90$ V vs. SCE) results in the loss of the ZW1 features in both the absorption and fluorescence spectra. Indeed, for an applied current of 1F, the electrolyzed solution becomes non-fluorescent, as expected for the resulting product MC2. Furthermore, the recovery of the fluorescence behavior of the sample, that is, the conversion of MC2 back into ZW1, is quantitatively achieved when an oxidation potential ($E = 1.20$ V vs. SCE, 1F) is subsequently applied to the sample (data not shown). Interestingly, successive application of such electrochemical fluorescent switching cycles does not result in a significant degradation of the system, as illustrated in Figure 8. Thus, upon three repeated reduction/oxidation cycles of ZW1 in acetonitrile, about 90% of the initial fluorescence signal is recovered. This allows the ZW1–MC2 couple to be envisaged as a versatile and stable fluorescent switching system, which can actuate upon both chemical and electrochemical stimuli. Indeed, although a variety of fluorescent redox-[25a,30] and pH-driven[31] switches are found in the literature, the design and characterization of molecular switches responding to both types of stimuli has scarcely been reported.[32]

Fluorescence switching at the single molecule level: Application of molecular switches at the nanometer scale will ultimately imply addressing their behavior at the single-molecule level. Herein we have analyzed the performance of the

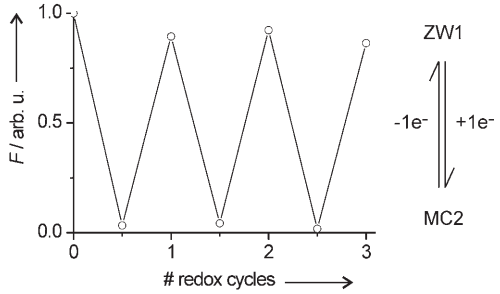

Figure 8. Fluorescence intensity at $\lambda_{em}=563$ nm of an acetonitrile solution of ZW1 ($c_{ZW1}=1\times10^{-5}$ M) upon consecutive reduction–oxidation cycles. The reduction and oxidation processes were performed by applying a current of 1 *F* at −0.9 and 1.2 V versus SCE, respectively.

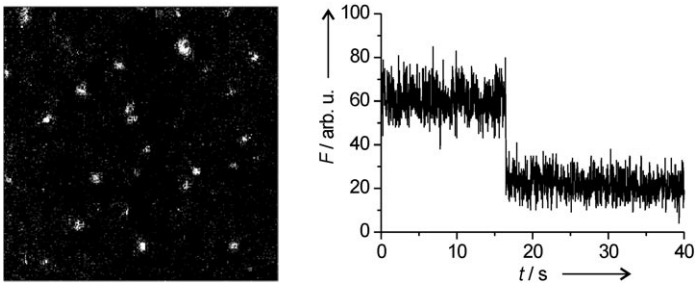

Figure 9. Fluorescence image (left) of a 10 μm × 10 μm area of a thin PS film with embedded ZW1 molecules ($\lambda_{exc}=532$ nm, power density ≈4 kW cm^{-2}, pixel rate = 0.5 kHz). Fluorescence intensity trajectory (right) of a single ZW1 molecule of the same sample upon continuous laser irradiation ($\lambda_{exc}=532$ nm, power density ≈4 kW cm^{-2}, integration time = 25 ms). The signal after $t=16$ s corresponds to the background of the detector at the current experimental conditions.

ZW1–MC2 pair as a true single-molecule fluorescent switch by means of single-molecule fluorescence spectroscopy.

Due to the high absorption cross-section and fluorescence quantum yield measured for ZW1 in acetonitrile, achieving detection of the fluorescence state of the switch at the single-molecule level is expected. The capability of SMS to reach this limit was explored on thin polystyrene films (PS, ≈40 nm thick) doped with ZW1 molecules by means of a custom-made confocal scanning fluorescence microscope. Figure 9 shows the fluorescence image registered for a 10 μm × 10 μm area of one of these samples. Comparison with the results obtained for similar non-doped PS films allows us to assign the bright features in the image to the emission arising from single immobilized ZW1 molecules. Figure 9 also depicts the fluorescence intensity time trajectory measured for an individual spot in the image upon continuous laser irradiation. Clearly, single step photo-bleaching of the emission occurs after 16 s, as similarly observed for most of the fluorescence features analyzed. This further proves the single emitter behavior of the bright spots detected for the ZW1@polystyrene samples, thus substantiating the potential of SMS to investigate the performance of individual ZW1–MC2 molecular switches.

Employing SMS we addressed the switching behavior of the ZW1–MC2 system at the single-molecule level upon acid–base-induced protonation–deprotonation of the Meisenheimer complexes. With this aim in view, we dispersed ZW1 molecules onto thin PS films (≈250 nm thick) supported on clean microscope coverglasses. This allows for: 1) direct exposure of the ZW1–MC2 molecules to several different atmospheres (acid, base, and neutral) with which the switching operation will be induced; and 2) prevention of the interaction of ZW1–MC2 molecules with either metallic impurities (e.g. TiO_2, Al_2O_3) or protonated sites on the surface of the coverglass. The binding of these species to the guanidine group of MC2 may interfere with the switching mechanism, as previously observed for another PET-driven molecular switch system.[15]

Figure 10 summarizes the results obtained on the single-molecule study of the acid–base switching performance of the ZW1–MC2 system. All six images displayed in Figure 10 were measured on the same sample upon successive expo-

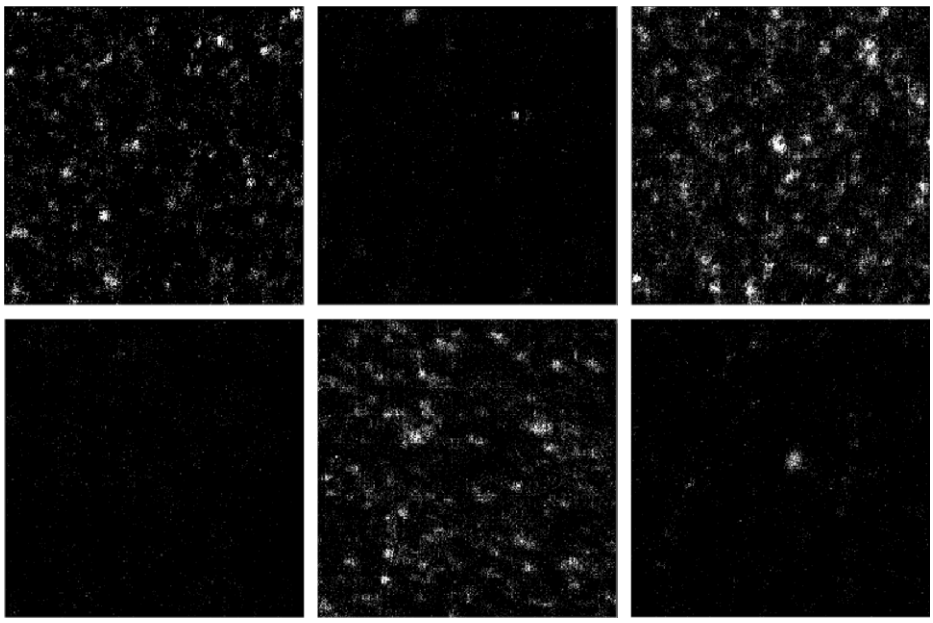

Figure 10. Fluorescence images of 10 μm × 10 μm areas of a thin PS film with ZW1 molecules on top after successive exposure of the sample to: air (top left); TEA/N_2 flow for 2 min (top middle); air for 30 min (top right); TEA/N_2 flow for 2 min (bottom left); HAc/N_2 flow for 30 s (bottom middle); TEA/N_2 flow for 2 min (bottom right). All six images were recorded with the same instrument settings ($\lambda_{exc}=532$ nm, power density ≈4 kW cm^{-2}, pixel rate = 1 kHz). The fluorescence intensity scale is also equal for all displayed images ($I_{min}=2$ kcount s^{-1}; $I_{max}=15$ kcount s^{-1}).

sures to different environments. To prevent degradation of the microscope piezoscanner during this process, the sample was taken out and placed back in the microscope between consecutive images. Therefore, the images do not correspond to the same specific region of the sample, but to different nearby areas.

The top left panel in Figure 10 shows a $10\,\mu m \times 10\,\mu m$ fluorescence image of a freshly prepared sample, in which immobilized ZW1 molecules lie on a PS film under air. As previously observed for ZW1 molecules embedded into PS, isolated bright spots arising from the emission of individual ZW1 molecules are encountered. Exposure of this sample to a flow of triethylamine (TEA)/N_2 for two minutes suppresses most of the fluorescence features in the image, as illustrated by the top middle panel in Figure 10. In agreement with the behavior measured in acetonitrile solution, the interaction between TEA and ZW1 on the surface of the PS film results in deprotonation of the guanidinium moiety, thus yielding non-fluorescent MC2 molecules that cannot be detected by means of SMS. We ascribe the few remaining fluorescent spots in the image either to ZW1 molecules that are not deprotonated even under a large excess of TEA (as also observed to occur in acetonitrile solution) or to the very limited number of fluorescent impurities found for identically prepared PS thick films without dispersed ZW1 molecules (less than two impurity spots per $10\,\mu m \times 10\,\mu m$ area). Control experiments on the latter samples demonstrated that exposure to any of the gas flows used in our measurements did not result in the occurrence of new fluorescent impurities on the scanned areas.

Notably, after use of the TEA/N_2 flow, the fluorescence of the individual switch molecules on the PS film surface could be turned back on by direct exposure to air for 30 minutes. Desorption and evaporation of TEA to the atmosphere displaces the deprotonation equilibrium back and, therefore, accounts for the recovery of the fluorescent features. This situation is illustrated by the top right panel in Figure 10, which exhibits a similar number of individual ZW1 molecules as the initial fluorescence image. A new treatment of the sample with the TEA/N_2 flow again induces the conversion of the switch molecules into the MC2 state, thus explaining the absence of fluorescence features in the bottom left image in Figure 10. Instead of shifting the acid–base equilibrium back by direct exposure to air, a faster recovery of the fluorescence properties of the sample can be attained by employing an acetic acid (HAc)/N_2 flow. Indeed, after exposure of the sample to this flow for 30 s, the bottom middle fluorescence image in Figure 10 is registered, which clearly shows the presence of individual fluorescent ZW1 molecules. As already discussed above, exposing the sample to an excess of acid may result in degradation of the Meisenheimer complexes by protonation and subsequent decomposition of the nitro groups in the trinitrociclohexadiene unit. We observed the occurrence of such a degradation process for long exposure times of ZW1 single-molecule samples to the HAc/N_2 flow, as well as for very short exposure times to the more acidic HCl/N_2 flow. The bottom right image in Figure 10 finally demonstrates the deprotonation of ZW1 molecules and disappearance of fluorescence features as a consequence of a new treatment with the basic TEA/N_2 flow. The accomplishment of three reversible on-off fluorescent switching cycles of individual ZW1–MC2 molecules is therefore demonstrated by the SMS measurements displayed in Figure 10.

Conclusion

This contribution is devoted to the investigation of a new fluorescent molecular switch system, a spirocyclic Meisenheimer complex consisting of an anionic trinitrociclohexadiene unit linked to a triazene ring. Protonation of the guanidine moiety in the triazene ring gives rise to a fluorescence zwitterionic complex (ZW1), while deprotonation of this group results in a non-fluorescent anionic species (MC2). Examination of the molecular orbital energies of ZW1 and MC2 by means of density functional theory calculations has unraveled the underlying mechanism accounting for their opposite fluorescent behavior. Photoinduced electron transfer (PET) from the deprotonated guanidine moiety to the trinitrociclohexadiene fluorophore quenches the emission from MC2. The occurrence of this quenching mechanism is prevented by protonation of the guanidine group, thus explaining the fluorescent properties of ZW1.

Spectrophotometric measurements in the bulk demonstrate that the on-off fluorescence switching between the ZW1 and MC2 states is achieved upon acid–base addition. Indeed, careful and controlled addition of these reactants allows the switching process to be fully reversible and repeatable. Moreover, we have also observed that transformation of the non-fluorescent MC2 species into a fluorescent Meisenheimer complex can be achieved by binding of other Lewis acids distinct from protons to the guanidine moiety of the system, thus allowing sensing of several different compounds. More importantly, combined spectroelectrochemical experiments in the bulk reveal that the fluorescent ZW1–MC2 switch can also operate under redox stimuli. Therefore, the ZW1–MC2 couple constitutes one of the first examples of fluorescent molecular switches responding both to chemical and electrochemical actuation.

Finally, single-molecule fluorescence spectroscopy (SMS) has been used to investigate the switching behavior of individual molecules of ZW1–MC2. First, we have demonstrated that, due to its high absorption cross-section and fluorescence quantum yield, the fluorescence from isolated single ZW1 complexes can be detected by means of SMS. Successive exposure of these molecules to basic, neutral, and acid gas flows has subsequently allowed us to monitor the reversible and controlled fluorescent switching of individual Meisenheimer complexes. In conclusion, the versatile functioning of the ZW1–MC2 couple upon different external stimuli as well as the capability of monitoring its switching operation at the single-molecule level allows one to envisage future applications of this system both as a single-molecule

probe of relevant chemical and biological processes and as a single-molecule switch in true nanometer sized devices.

Experimental Section

Materials and synthesis: High purity chemicals and HPLC-grade solvents were used in all bulk measurements and single-molecule sample preparation, and were used as purchased, without further purification. The synthesis and structural characterization of ZW1[18] and MC2[21] have already been reported.

Steady-state absorption and fluorescence spectroscopy: UV/Vis spectra were recorded at room temperature using a HP 8452 A Spectrophotometer with chemstation software. Fluorescence spectra were recorded at room temperature in a Perkin Elmer Luminescence Spectrometer LS50. The fluorescence quantum yields of ZW1 and MC2 in acetonitrile were determined relative to *N,N′*-bis(1-hexylheptyl)perylene-3,4,9,10 tetracarboxybismide in acetonitrile ($\Phi_f = 1$).[33]

Theoretical methods: Quantum-chemical calculations were performed by employing the Gaussian 03 package of programs[34] on a 32-bit multiprocessor computer. Density functional theory (DFT) geometrical optimization of ZW1 and MC2 ground electronic states was carried out at the B3LYP hybrid functional level with the 6–31G(d,p) basis set. To account for solvent polarity effects, calculations were performed in acetonitrile solvent by means of the polarizable continuum model (PCM, dielectric constant = 36.64). The molecular orbitals of the computed ground state geometries were calculated with the larger 6–311G+(d,p) basis set and plotted using Molden. The excitation energies and oscillator strengths (f) of the UV/Vis absorption transition bands of ZW1 and MC2 were computed by means of time-dependent density functional theory at the B3LYP/6–311G+(d,p) level on the B3LYP/6–31G(d,p) ground state geometries and accounting for acetonitrile solvent (PCM). To compare with experimental data, only those transitions with $f > 0.05$ were considered.

Spectrophotometric measurements of the acid–base switching: A solution of ZW1 (10^{-4}–10^{-5} M) in acetonitrile (4 mL) was prepared and successive and controlled additions of base (tetrabutylammonium hydroxide in 2-propanol) and acid (perchloric acid in dioxane) to this solution were performed. Absorption and fluorescence spectra were measured after each addition employing the above-mentioned spectrophotometric instruments at room temperature.

Spectroelectrochemistry measurements of the redox switching: A solution of ZW1 or MC2 (1–5 mM) in acetonitrile (5 mL), containing 0.1646 g of NBu_4BF_4 (0.1 M) as supporting electrolyte, was prepared under an argon atmosphere. A reductive controlled-potential electrolysis at −0.90 V versus SCE or oxidative controlled-potential electrolysis at 1.20 V versus SCE were performed by using a carbon graphite rod as a working electrode in a dark electrochemical cell for converting ZW1 into MC2 or MC2 into ZW1, respectively. After application of several increasing values of current (from 0 to 1 F) the absorption and fluorescence spectra of the resulting sample was measured in the above-mentioned spectrophotometric instruments at room temperature.

Single-molecule fluorescence spectroscopy measurements: Single-molecule fluorescence experiments were performed on a home-built confocal scanning fluorescence microscope. This instrument consists of a high-NA oil-immersion objective (Olympus, 60×, NA = 1.42) mounted on an inverted focusing unit (Olympus, BXFM), with which the circularly polarized light from a continuous green diode laser ($\lambda = 532$ nm, Z-laser, Z20RG) is focused onto the sample. The resulting fluorescence emission is collected by the same objective, spectrally filtered from excitation light using dichroic (Omega, 550DRLP) and long-pass (Omega, 550 ALP) filters, and finally detected in an avalanche photodiode (Perkin-Elmer, SPCM-AQR-14). Fluorescence images were obtained by raster-scanning 10 μm × 10 μm areas of the samples by means of a piezoscanner with position feedback control (Physik, Instrumente, P-710) at 0.5–1 kHz pixel rate and with a laser excitation power density of about 4 kW cm^{-2}. The movement of the scanner as well as the collection of the signal of the photodetector is controlled by means of a LabVIEW (National Instruments) program. Two different types of samples were measured on this instrument: 1) thin polymer films (≈40 nm) with embedded ZW1 molecules, which were obtained by spin-coating a toluene solution of ZW1 (≈10^{-9} M) and polystyrene ($M_w = 97400$, Aldrich, 10 g L^{-1}) onto a microscope coverglass; 2) thin polymer films (≈250 nm) with dispersed ZW1 molecules on top, which were prepared by sequentially spin-coating a toluene solution of polystyrene (40 g L^{-1}) and an ethanol solution of ZW1 (≈10^{-9} M) onto a microscope coverglass. The thicknesses of the polymer films were measured with a surface profiler (KLA-Tencor, Alpha IQ). Fluorescent impurities on the surface of the microscope coverglasses were removed upon heating in an oven at 450 °C for 30 min. Switching of the individual ZW1 and MC2 molecules in type (2) samples was induced by exposure to triethylamine/N_2, air or acetic acid/N_2 flows in the interior of a homebuilt gas chamber.

Acknowledgements

The authors thank Prof. Dr. M. Blanco (Universitat Autònoma de Barcelona) for the use of the fluorescence spectrophotometer and Mr. G. Sánchez-Mosteiro (Institut de Ciències Fotòniques) for polymer film thickness measurements. This work has been supported by the Spanish Ministry for Education and Science through projects CTQ2006–01040, CTQ2005–09334-C02 and the "Ramon y Cajal" program (J.H.). Financial support from the Marie-Curie program of the European Commission through project MERG-CT-2004–513601 is also acknowledged.

[1] a) *Molecular Switches* (Ed.: B. Feringa), Wiley-VCH, Weinheim, **2002**; b) V. Balzani, M. Venturi, A. Credi, *Molecular Devices and Machines: A Journey into the Nanoworld*, Wiley-VCH, Weinheim, **2003**.

[2] A. P. de Silva, H. Q. M. Gunaratne, T. Gunnlaugsson, A. J. M. Huxley, C. P. McCoy, J. T. Rademacher, T. E. Rice, *Chem. Rev.* **1997**, *97*, 1515–1566.

[3] Special Issue: Photochromism: Memories and Switches, *Chem. Rev.* **2000** (Guest Ed.: M. Irie), *100*, 1683–1890.

[4] a) R. A. Bissell, E. Cordova, A. E. Kaifer, J. F. Stoddart, *Nature* **1994**, *369*, 133–137; b) T. Hugel, N. B. Holland, A. Cattani, L. Moroder, M. Seitz, H. E. Gaub, *Science* **2002**, *296*, 1103–1106; c) R. Hernandez, H. R. Tseng, J. W. Wong, J. F. Stoddart, J. I. Zink, *J. Am. Chem. Soc.* **2004**, *126*, 3370–3371; d) J. D. Badjic, V. Balzani, A. Credi, S. Silvi, J. F. Stoddart, *Science* **2004**, *303*, 1845–1849.

[5] a) C. Joachim, J. K. Gimzewski, A. Aviram, *Nature* 2000, 408, 541–548; b) Z. J. Donhauser, B. A. Mantooth, K. F. Kelly, L. A. Bumm, J. D. Monnell, J. J. Stapleton, D. W. Price, A. M. Rawlett, D. L. Allara, J. M. Tour, P. S. Weiss, *Science* **2001**, *292*, 2303–2307; c) F. Moresco, G. Meyer, K. H. Rieder, H. Tang, A. Gourdon, C. Joachim, *Phys. Rev. Lett.* **2001**, *86*, 672–675.

[6] a) T. Basché, W. E. Moerner, *Nature* **1992**, *355*, 335–337; b) F. Kulzer, S. Kummer, R. Matzke, C. Bräuchle, T. Basché, *Nature* **1997**, *387*, 688–691; c) F. Kulzer, M. Orrit, *Ann. Rev. Phys. Chem.* **2004**, *55*, 585–611; d) M. Sauer, *Proc. Natl. Acad. Sci. USA* **2005**, *102*, 9433–9434.

[7] a) T. Basché, W. E. Moerner, M. Orrit, U. P. Wild, in *Single-molecule Optical Detection, Imaging and Spectroscopy*, VCH Publishers, Berlin, **1996**; b) W. E. Moerner, M. Orrit, *Science*, **1999**, *283*,1670–1675.

[8] a) M. Irie, T. Fukaminato, T. Sasaki, N. Tamai, T. Kawai, *Nature* **2002**, *355*, 335–337; b) T. Fukaminato, T. Sasaki, T. Kawai, N. Tamai, M. Irie, *J. Am. Chem. Soc.* **2004**, *126*, 14843–14849.

[9] M. Heilemann, E. Margeat, R. Kasper, M. Sauer, P. Tinnefeld, *J. Am. Chem. Soc.* **2005**, *127*, 3801–3806.

[10] M. Bates, T. R. Blosser, X. Zhuang, *Phys. Rev. Lett.* **2005**, *94*, 108101.

[11] R. M. Dickson, A. B. Cubitt, R. Y. Tsien, W. E. Moerner, *Nature* **1997**, *388*, 355–358.

[12] S. Habuchi, R. Ando, P. Dedecker, W. Verheijen, H. Mizuno, A. Miyawaki, J. Hofkens, *Proc. Natl. Acad. Sci. USA* **2005**, *102*, 9511–9516.
[13] J. J. La Clair, *Angew. Chem.* **1999**, *111*, 3231–3233; *Angew. Chem. Int. Ed.* **1999**, *38*, 3045–3047.
[14] S. Brasselet, W. E. Moerner, Single Molecules **2000**, *1*, 17–23.
[15] L. Zang, R. Liu, M. W. Holman, K. T. Nguyen, D. M. Adams, *J. Am. Chem. Soc.* **2002**, *124*, 10640–10641.
[16] H. Neuweiler, A. Schulz, A. C. Vaiana, J. C. Smith, S. Kaul, J. Wolfrum, M. Sauer, *Angew. Chem.* **2002**, *114*, 4964–4968; *Angew. Chem. Int. Ed.* **2002**, *41*, 4769–4773.
[17] M. Sauer, *Angew. Chem.* **2003**, *115*, 1834–1837; *Angew. Chem. Int. Ed.* **2003**, *42*, 1790–1793.
[18] R. O. Al-Kaysi, G. Guirado, E. J. Valente, *Eur. J. Org. Chem.* **2004**, 3408–3411.
[19] F. Terrier in *Nucleophilic Aromatic Displacement* (Ed.: H. Feuer), VCH Publishers, New York, **1991**.
[20] S. Farnham, R. Taylor, *J. Org. Chem.* **1974**, *39*, 2446–2447.
[21] I. Gallardo, G. Guirado, *Electrochem. Commun.* **2007**, *9*, 173–179.
[22] M. J. Strauss, *Chem. Rev.* **1970**, *70*, 667–712.
[23] R. O. Al-Kaysi, D. Creed, E. J. Valente, *J. Chem. Crystallogr.* **2004**, *34*, 685–692.
[24] K. Tanaka, T. Miura, N. Umezawa, Y. Uranao, K. Kikuchi, T. Higuchi, T. Nagano, *J. Am. Chem. Soc.* **2001**, *123*,2530–2536.
[25] a) P. Yan, M. W. Holman, P. Robustelli, A. Chowdhury, F. I. Ishak, D. M. Adams, *J. Phys. Chem. B* **2005**, *109*, 130–137; b) M. W. Holman, P. Yan, K. C. Ching, R. C. Liu, F. I. Ishak, D. M. Adams, *Chem. Phys. Lett.* **2005**, *413*, 501–505.
[26] R. A. Bissell, A. P. de Silva, H. Q. N. Guanaratne, P. L. M. Lynch, G. E. M. Maguire, C. P. McCoy, K. R. A. S. Sandanayake, *Top. Curr. Chem.* **1993**, *168*, 223–264.
[27] a) W. Huber, in *Titration in non-aqueos solvents*, Academic Press Inc., New York, **1967**; b) J. S. Fritz, *Anal. Chem.* **1953**, *25*, 407–411; c) S. Serin, M. Kurtuglu, *Analyst*, **1994**, *119*, 2213–2215; d) T. Gunduz, E. Kilic, G. Ozkan, M. F. Award, M. Tastein, *Anal. Chim. Acta* **1990**, *234*, 339–344.
[28] G. A. Artamkina, M. P. Egorov, I. P. Beletskaya, *Chem. Rev.* **1982**, *82*, 427–459.
[29] H. Langhals, W. Jona, *Chem. Eur. J.* **1998**, *4*, 2110–2116.
[30] a) V. Goulle, A. Harriman, J.-M. Lehn, *J. Chem. Soc. Chem. Commun.* **1993**, 1034–1036; b) J. Daub, B. Martin, A. Knorr, H. Spreitzer, *Pure Appl. Chem.* **1996**, *68*, 1399–1404; c) L. Fabbrizzi, M. Licchelli, P. Pallavicini, *Acc. Chem. Res.* **1999**, *32*, 846–853; d) H. Li, J. O. Jeppesen, E. Levillain, J. Becher, *Chem. Commun.* **2003**, 846–847; e) T. Suzuki, A. Migita, H. Higuchi, H. Kawai, K. Fujiwara, T. Tsuji, *Tetrahedron Lett.* **2003**, *44*, 6837–6840; f) R. Martínez, I. Ratera, A. Tàrraga, P. Molina, J. Veciana, *Chem. Commun.* **2006**, 3809–3811.
[31] a) A. P. de Silva, H. Q. N. Gunaratne, C. P. McCoy, *Chem. Commun.* **1996**, 2399–2400; b) R. P. Haugland in *Handbook of Fluorescent Probes and Research Products*, Molecula Probe, Eugene, **2002**; c) Y.-D. Cao, Q.-Y. Zheng, C.-F. Chen, Z.-T. Huang, *Tetrahedron Lett.* **2003**, *44*, 4751–4755; d) J. F. Callan, A. P. de Silva, N. D. McClenaghan, *Chem. Commun.* **2004**, 2048–2049; e) Y. Shiraishi, Y. Tokitoh, G. Nishimura, T. Hirai, *Org. Lett.* **2005**, *7*, 2611–2614; f) M. Tomasulo, I. Yildiz, S. L. Kaanumalle, F. M. Raymo, *Langmuir* **2006**, *22*, 10284–10290.
[32] H. Rohr, C. Trieflinger, K. Rurack, J. Daub, *Chem. Eur. J.* **2006**, *12*, 689–700.
[33] T. Kircher, H.-G. Löhmannsröben, *Phys. Chem. Chem. Phys.* **1999**, *1*, 3987–3992.
[34] Gaussian 03 (Revision B.04), M. J. Frisch, G. W. Trucks, H. B. Schlegel, G. E. Scuseria, M. A. Robb, J. R. Cheeseman, J. A. Montgomery, Jr., T. Vreven, K. N. Kudin, J. C. Burant, J. M. Millam, S. S. Iyengar, J. Tomasi, V. Barone, B. Mennucci, M. Cossi, G. Scalmani, N. Rega, G. A. Petersson, H. Nakatsuji, M. Hada, M. Ehara, K. Toyota, R. Fukuda, J. Hasegawa, M. Ishida, T. Nakajima, Y. Honda, O. Kitao, H. Nakai, M. Klene, X. Li, J. E. Knox, H. P. Hratchian, J. B. Cross, V. Bakken, C. Adamo, J. Jaramillo, R. Gomperts, R. E. Stratmann, O. Yazyev, A. J. Austin, R. Cammi, C. Pomelli, J. W. Ochterski, P. Y. Ayala, K. Morokuma, G. A. Voth, P. Salvador, J. J. Dannenberg, V. G. Zakrzewski, S. Dapprich, A. D. Daniels, M. C. Strain, O. Farkas, D. K. Malick, A. D. Rabuck, K. Raghavachari, J. B. Foresman, J. V. Ortiz, Q. Cui, A. G. Baboul, S. Clifford, J. Cioslowski, B. B. Stefanov, G. Liu, A. Liashenko, P. Piskorz, I. Komaromi, R. L. Martin, D. J. Fox, T. Keith, M. A. Al-Laham, C. Y. Peng, A. Nanayakkara, M. Challacombe, P. M. W. Gill, B. Johnson, W. Chen, M. W. Wong, C. Gonzalez, J. A. Pople, Gaussian, Inc., Wallingford CT, **2004**.

Received: February 9, 2007
Revised: April 12, 2007
Published online: June 22, 2007

